Seasonal Cycle of Sea Surface Salinity in the Angola Upwelling System

F. M. Awo, M. Rouault, M. Ostrowski, F. S. Tomety, C. Y. Da-Allada, J. Jouanno

JGR Oceans

RESEARCH ARTICLE
10.1029/2022JC018518

Key Points:

- The surface salinity along the Angolan coast presents a semi-annual cycle
- The Angola Current drives the low-salinity intrusion at the Angolan coast while subsurface processes bring salty water toward the surface
- The low-salinity intrusion at the Angolan coast creates a strong vertical salinity gradient that favors vertical salt advection

Correspondence to:
F. M. Awo,
mesmin.awo@gmail.com

Citation:
Awo, F. M., Rouault, M., Ostrowski, M., Tomety, F. S., Da-Allada, C. Y., & Jouanno, J. (2022). Seasonal cycle of sea surface salinity in the Angola upwelling system. *Journal of Geophysical Research: Oceans*, *127*, e2022JC018518. https://doi.org/10.1029/2022JC018518

Received 6 FEB 2022
Accepted 15 JUN 2022

Author Contributions:
Conceptualization: F. M. Awo, M. Rouault
Data curation: J. Jouanno
Formal analysis: F. M. Awo, M. Rouault, F. S. Tomety, C. Y. Da-Allada
Funding acquisition: M. Rouault, M. Ostrowski
Investigation: F. M. Awo, M. Rouault, M. Ostrowski, F. S. Tomety, C. Y. Da-Allada, J. Jouanno
Methodology: F. M. Awo
Software: F. M. Awo
Supervision: M. Rouault, M. Ostrowski
Validation: F. M. Awo, M. Rouault
Visualization: F. M. Awo, F. S. Tomety
Writing – original draft: F. M. Awo
Writing – review & editing: F. M. Awo, M. Rouault, M. Ostrowski, F. S. Tomety, C. Y. Da-Allada, J. Jouanno

Seasonal Cycle of Sea Surface Salinity in the Angola Upwelling System

F. M. Awo[1,2], M. Rouault[1], M. Ostrowski[3], F. S. Tomety[1], C. Y. Da-Allada[2,4], and J. Jouanno[5]

[1]Nansen-Tutu Centre for Marine Environmental Research, Department of Oceanography, University of Cape Town, Cape Town, South Africa, [2]ICMPA-UNESCO Chair/UAC, Cotonou, Bénin, [3]Institute of Marine Research (IMR), Bergen, Norway, [4]LaGEA/ENSTP/UNSTIM, Abomey, Bénin, [5]LEGOS, CNES/CNRS/IRD/UPS, Toulouse, France

Abstract The seasonal cycle of sea surface salinity (SSS) along the Angolan coast is investigated using observations and a regional ocean model. The model reproduces the main characteristic of the seasonal cycle of SSS along the Angolan coast, such as the freshwater discharge signature off the Congo River plume and the low-salinity observed in February/March and October/November along the Angolan coast. The model also reproduces the two maxima of salinity in June/July and December/January. The analysis of the model salt budget reveals that the semi-annual cycle of SSS is controlled by the meridional advection of surface water, the vertical advection of subsurface water, and the mixing at the base of the mixed layer. The meridional advection is controlled by the Angola Current which brings low-salinity water from offshore region of the Congolese coast toward the south Angolan coast in February/March and October/November. The vertical advection contribution is modulated by the vertical stratification of salinity and not by vertical velocities which peak during the main Angolan upwelling season. The vertical stratification is due to the low-salinity intrusion at the Angolan coast that creates a strong vertical salinity gradient with low-salinity at the surface and high salinity at the subsurface.

Plain Language Summary Ocean salinity is a key driver of oceanic circulation, and it affects profoundly the marine coastal ecosystem. We study here the seasonal cycle of the upper ocean salinity off the Angolan coast. We observe a low-salinity water intrusion in February/March and October/November along the Angolan coast. We find the low-salinity intrusion due to the well-known Angola Current that brings low-salinity waters from the Congo River plume southward. On its way south along the Angola coast, surface water gains salt from subsurface water that rises to the surface through upwelling and mixing at the base of the ocean surface mixed layer.

1. Introduction

The Angolan upwelling region is a very productive marine ecosystem in the southeast Atlantic and serves as the gateway for connecting the equatorial dynamics to the northern Benguela. Fisheries are widely developed along the Angolan shore and are critical for economic security and the employment of local coastal communities (Hutchings et al., 2009; Sowman & Cardoso, 2010). Contrary to the Benguela upwelling system that is sustained by high alongshore upwelling favorable winds (Carr & Kearns, 2003), the highly productive Angolan system is under the influence of relatively weak surface winds blowing along the coast (Blamey et al., 2015; Hellerman, 1980; Ostrowski et al., 2009) and of the Angolan Current that transports warm equatorial waters southward (Kopte et al., 2017; Moroshkin et al., 1970). The Angola upwelling system is supported by the poleward propagation of coastal trapped waves originating from the equator (Bachèlery et al., 2016, Illig et al., 2020; Imbol Koungue et al., 2017), which strongly modulate the strength of the Angola Current (Ostrowski et al., 2009; Rouault, 2012). The main Angolan upwelling season is in austral winter with sea surface temperatures below 22.5°C in July along the coast and a marked cross-shore SST thermal gradient (Figures 1a and 1b). In July, the salinity is relatively high with a surface salinity above 36 along the Angolan coast and the Congo freshwater plume with surface salinity below 35 presents a minimal offshore extension that is directed toward the northwest (Figures 1c and 1d). The two main regimes of the freshwater Congo River plume spreading at the Congolese coast are a north-westward orientated plume from September to January and a south-westward plume from January to April (Houndegnonto et al., 2021).

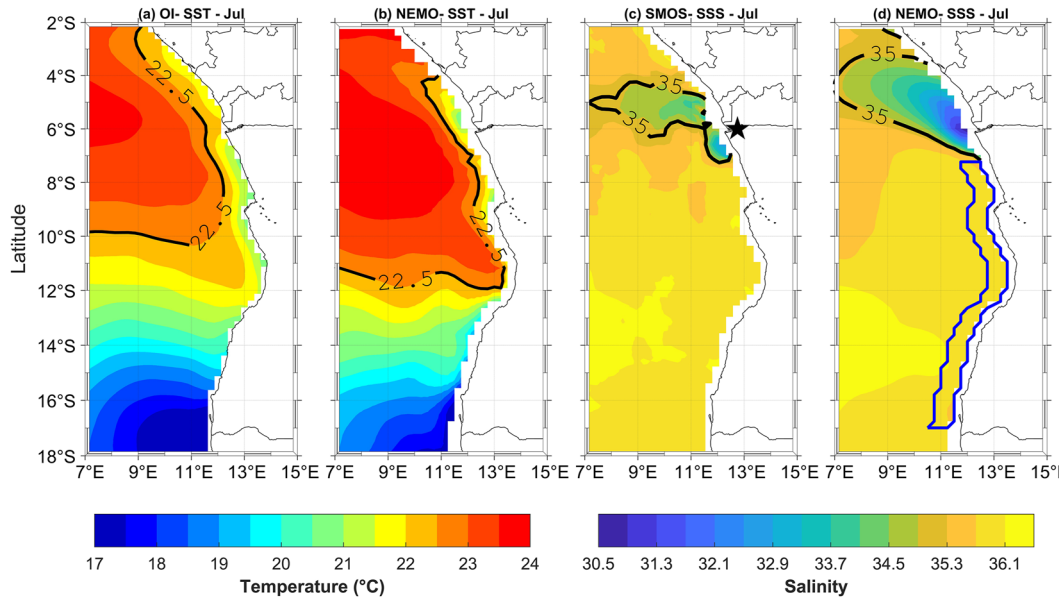

Figure 1. Climatological Sea Surface Temperature (a, b) and Salinity (c, d) averaged in July from the derived satellite Optimal Interpolation (a, -OI-), SMOS (c) and the model (b, d) over the period 1982–2015 for the model, 1982–2021 for OI, and 2010–2021 for SMOS. The black star on Figure 1c (at 6.2°S, 12°E) represents the position of the Congo River mouth. The 1° wide coastal stripe off the Angolan coast used in the study is represented by the blue contour line on Figure 1d (1° off the coast, 7°S–17°S).

Lübbecke et al. (2019) have shown that for the warm event in 2016 off Angola, surface freshening of water originating from the Congo River plume, detected in satellite observations of sea surface salinity (SSS), caused a very shallow mixed layer, and enhanced upper ocean stratification that reduced the upwelling of cool subsurface water into the mixed layer. Moreover, Materia et al. (2012) had shown that years with increased Congo River discharge as well as years with anomalously high oceanic precipitation were associated with positive SST anomalies in the Gulf of Guinea. They attribute this relation to a strong stratification and specifically the development of a barrier layer due to the excess freshwater prevent turbulent mixing by vertical motion. The barrier layer then inhibits the entrainment of cool subsurface waters into the surface mixed layer, thereby increasing sea surface temperature. Recently, Alory et al. (2021) have shown at the seasonal timescale a limitation of the northeast Gulf of Guinea upwelling by the Niger River plume. There, the upwelling is weakened by 50% due to an onshore directed geostrophic flow equally controlled by alongshore thermosteric and halosteric sea-level changes. All these findings highlight the potential role of ocean salinity in the dynamic of coastal upwelling near a river plume. Several studies have investigated the seasonal cycle of salinity off the Congo River plume with model and observations analyses, however along the Angolan coast, studies are limited despite the possible link with the Congo River discharge (Lübbecke et al., 2019; Ostrowski et al., 2009). The studies of Camara et al. (2015) and Da-Allada et al. (2013, 2014) have widely investigated the various processes controlling seasonal cycle of the mixed-layer salinity budget in the Gulf of Guinea using a regional model (Figures 1b and 1d), with a special focus on the Congo River plume area. In the Congo River plume area, the regional model shows that the main salinity balance in the surface water is controlled by the salinization effects of vertical diffusion and vertical advection, and the freshening effects of horizontal advection and freshwaters fluxes composed mainly of Congo River runoff, which accounts for 80% of all freshwater input in this area.

While several studies have focused on the annual cycle of the SSS in the tropical Atlantic, they have not focused on the specific dynamics of the Angolan coastal region in relation with SSS. In this study, we use a regional model and satellited derived observational estimates to conduct an analysis of the seasonal cycle of the SSS along the Angolan coast and their drivers. The remainder of the paper is organized as follows. The data sets and methods used in the study are described in Section 2. Section 3 provides results, including model validation, the seasonal cycle of SSS along the coast and their drivers. Section 4 provides a summary of the most important results.

2. Data and Methods

For the analysis, satellite data, reanalysis data, and a regional numerical model simulation are used.

2.1. Data

2.1.1. Satellite Data

An updated version of the Soil Moisture-Ocean Salinity (SMOS) product described in Boutin et al. (2022) is used. This ¼° weekly gridded product covering the period 2010–2021 is made available after the systematic coastal biases have been removed within 100 km from the coast (Kolodziejczyk et al., 2016). A previous version of the SMOS product has been used and described in our previous study (Awo et al., 2018). The monthly average of the daily Optimum Interpolation Sea Surface Temperature (OI-SST) is also used and consists of a blend of satellite and in situ observations. The daily OI-SST data is available from July 1981 to December 2021 at a spatial resolution of 0.25° (Reynolds et al., 2002, 2007). The current data set is provided by Ocean Surface Current Analysis (OSCAR) for the time period 1993–2020. The OSCAR data set provides a near-surface currents on a 0.25° by 0.25° horizontal grid with a daily temporal resolution. The data is estimated from satellite remote sensing estimates of sea surface height gradients, ocean vector winds, and SST gradient using a simplified physical model for geostrophy, Ekman, and thermal wind dynamics (Bonjean & Lagerloef, 2002; ESR & Dohan, 2022). The total velocity of the current is the vertical average over a surface layer thickness of 30 m. The AVISO monthly seasonal cycle of sea level anomaly (SLA) based on the period 1993–2021 is also used to illustrate the propagation of coastal trapped waves. We refer to all satellite data sets as observations and will use them for model validation in Section 3.1.

2.1.2. Reanalysis Products

The monthly wind product is derived from the European Center for Medium Range weather Forecasts ERA5 reanalysis (Hersbach et al., 2020). We used the full monthly average data over the 1979–2021 period.

2.1.3. Mooring Data

A current meter mooring has been deployed at about 11°S off the Angolan coast since 2013 to measure the current speed in the water column up to about 45 m below the sea surface (Imbol Koungue et al., 2021; Kopte et al., 2017). The current velocity is measured by an ADCP mounted on the mooring cable at 500 m depth with an upward looking 75 kHz long Ranger up to 45 m below the sea surface. The mooring data is freely available from July 2013 to May 2021 (Imbol Koungue et al., 2021).

2.1.4. Model

The ocean general circulation model used here is the oceanic component of the Nucleus for European Modeling of the Ocean (NEMO3.6, Madec & the NEMO group, 2016). It tackles three-dimensional primitive equations in spherical coordinates discretized on a C-grid and at fixed vertical levels. The exact model domain covers the tropical Atlantic (34°S–34°N, 50°W–20°E) and is forced at the open ocean boundaries with daily outputs of the second global ocean Mercator reanalysis version 3 (GLORYS2V3; Ferry et al., 2012). We used here the monthly outputs of the regional model configuration that covers the tropical Atlantic with a spatial resolution of 0.25° × 0.25°. The model has 75 vertical levels of which 12 are located in the upper 20 m and 24 in the upper 100 m. The salt mixed layer budget terms are computed online with daily average outputs. The model has been run from 1958 to 2015, however only outputs from the period 1982–2015 are used in this study so that they can be compared with observations. This setup has been used previously for salinity studies by Awo et al. (2018) and Da-Allada et al. (2017) in the tropical Atlantic. The atmospheric fluxes of momentum, heat, and freshwater are provided by bulk formulae (Large & Yeager, 2004). The DRAKKAR Set 5.2 (DFS5.2) product of fields for wind, atmospheric temperature, humidity, and fields for long and short-wave radiation and precipitation are used to force the model (Dussin et al., 2016). There is neither SSS restoring nor SST restoring in this simulation. The monthly continental river discharge climatology is used for the surface freshwater flow near each River mouth (Berger et al., 2014; Dai & Trenberth, 2002). For more details on the parameterization of subgrid scale processes and some validation elements, reference can be made to Hernandez et al. (2017), Imbol Koungue et al. (2019), and Jouanno et al. (2017) for temperature and mixed layer depth and Awo et al. (2018) for salinity variations.

2.2. Methods

To obtain a consistent monthly climatology time-series for the study, we used the entire available satellite observation for SMOS (2010–2021) and OI-SST (1982–2021). For NEMO model output, we used the period 1982–2015.

We used the mixed-layer salinity budget terms computed online and saved as model output to investigate the processes driving the seasonal cycle of SSS. The mixed-layer budget analysis has been widely used in ocean surface processes studies, for instance within the tropical Atlantic, for SST (e.g., Jouanno et al., 2017, 2011) and for SSS (Awo et al., 2018; Berger et al., 2014; Camara et al., 2015; Da-Allada et al., 2014, 2017). For the SSS budget, we relied on the common following mixed-layer salinity evolution equation:

$$\partial_t \mathrm{SSS} = \underbrace{- < u\partial_x S >}_{\mathrm{UAD}} \underbrace{- < v\partial_y S >}_{\mathrm{VAD}} \underbrace{- < w\partial_z S >}_{\mathrm{WAD}} \underbrace{+ < D_l S >}_{\mathrm{LDIF}} \underbrace{- \frac{(k_z \partial_z S)_{z=-h}}{h}}_{\mathrm{VDIF}} \underbrace{- \frac{1}{h}\frac{\partial h}{\partial t}(\mathrm{SSS} - S_{z=-h})}_{\mathrm{ENT}} + \underbrace{\frac{(E-P-R)\mathrm{SSS}}{h}}_{\mathrm{FWF}}$$

with $< . >= \frac{1}{\mathbf{h}} \int . \mathbf{dz}$

where S is the model salinity and u, v, and w are the components of the current in the zonal (positive eastward), meridional (positive northward), and vertical (positive upward) direction, respectively. ($D_l S$) is the lateral diffusion operator, k_z is the vertical diffusion coefficient, h is the mixed-layer depth, E is evaporation, P is precipitation, and R is River runoff. The terms in the equation are, from left to right, salinity tendency in the mixed layer, contribution to mixed-layer salinity tendency of the zonal advection (UAD), meridional advection (VAD), vertical advection (WAD), horizontal diffusion (LDIF), vertical diffusion at the mixed-layer base (VDIF), mixed-layer salinity tendency due to entrainment at the mixed-layer base (ENT), and freshwater flux (FWF). We mean by salinity tendency, the rate of salinity changes from 1 month to the next. All terms are computed explicitly in the model except for the entrainment term that is estimated as a residual.

3. Results

The entire Angola coastal area (7°S−17°S, 1°offshore, Figure 1d) is considered to analyze the seasonal cycle of SSS in the Angolan Upwelling system. The North Angola area (7°S–10°S) corresponds to the northern part of the Angolan upwelling that could be directly under the influence of the Congo River plume extension. The South Angola area (10°S–17°S) corresponds to the southern part of the Angolan upwelling that could not be directly influenced by the Congo River plume and is also well-known as a key area for the development of Benguela Niños events (Florenchie et al., 2004; Imbol Koungue et al., 2017; Lübbecke et al., 2010; Rouault, 2012; Shannon et al., 1986).

3.1. Model Validation

Figure 2 shows the model and observed seasonal cycles of the SST, SSS, wind speed, SLA and the near-surface current along the Congolese coast (4°S–6°S, 1°offshore) and Angolan coast (7°S–17°S, 1°offshore). The seasonal cycle along the coasts is characterized by four specific seasons: austral winter (June–July–August), austral spring (September–October–November), austral summer (December–January–February), and austral autumn (March–April–May). The Angola upwelling peaks in austral winter as illustrated by observed coastal temperatures below 22.5°C in July–August (Figures 2a and 2b) with an important cross-shore SST gradient in July (Figure 1a). The seasonal cycle of SSS along the coasts presents a semi-annual cycle south of 7°S with a main salinity maximum of 36 in austral winter, in phase with the cool SST and a secondary maximum of 35.5 in November–December. In the northern part of the Angola coast, the SSS falls below 31 near the Congo River plume (6°S, 8°E) revealing the signature of the Congo River freshwater discharge. There, the low-salinity below 31 is observed from September to April and increases to 35 in austral winter.

The regional simulation reproduces the main pattern of the observed seasonal cycle of SST (Figure 2b) and SSS (Figure 2e) along the Angolan and Congolese coasts. The SST is relatively well captured by the model with the warmest water of temperature above 28°C in autumn (Figure 2b) and the coolest upwelling water of temperature below 22.5°C in winter. The model also captures relatively well the SSS by reproducing the mean and phase of the observed seasonal cycle previously described. The modeled temperature is higher than observed SST with an SST difference of about 1°C while the model salinity is lower than observation with an SSS difference about

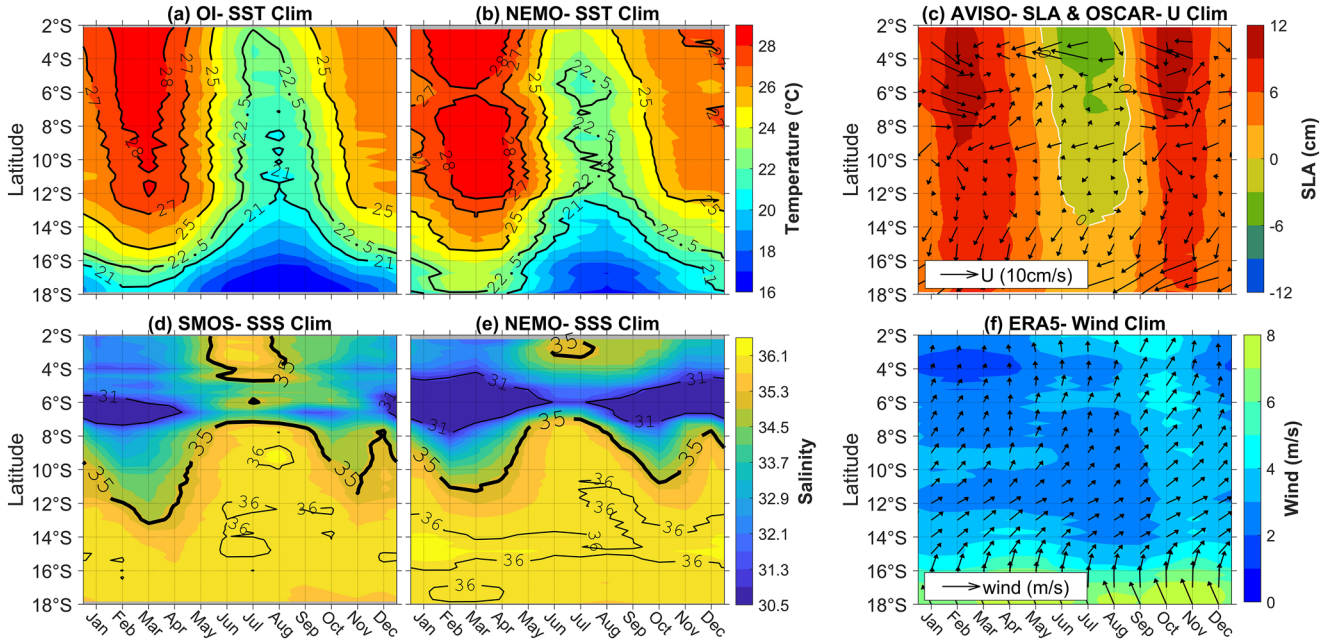

Figure 2. Latitude-time Hovmöller diagram of seasonal cycle of OI SST (a), NEMO SST (b), SMOS SSS (d), NEMO SSS (e), AVISO SLA (c), OSCAR current (arrow, c) and ERA5 wind speed (shading and arrows, f) averaged over 1°off the coast from observations (a, c, d, f) and model (b, e). Unit are °C for SST, m for SLA, m/s for Wind speed and cm/s current velocity.

2 mainly in the northern part of Angolan coast. At the first order, the lack of accuracy in model river discharge may explain the weakness of the model in the northern part of the Angolan coast (Da-Allada et al., 2013, 2014) and the uncertain accuracy of the SMOS estimates in the river discharge area may bias the coastal SSS estimate (Boutin et al., 2018). In addition, inaccuracy of the mixed layer thickness and uncertainty in the wind stress forcing can also contribute to explaining the lack of accuracy in the model. Also note that the SMOS salinity delivers practical salinity defined as conductivity ratio while the model salinity is using mass conservation and therefore is not calculating the practical salinity but absolute salinity. In Figure 2, we also present the SLA (Figure 2c) and wind (Figure 2f) that influence the upwelling along the Congolese and Angolan coasts. The alongshore winds are weak in winter (June–August, Figure 2f) with an intensity of 2 m/s, suggesting that processes other than local wind-driven upwelling can explain the Angolan upwelling. The SLA along the coast is positive from September to April in the order of 10 cm with two maxima in spring and autumn and is negative from May to August in the order of −4 cm, with a minimum in winter during the major Angola upwelling. The SLA represents the signature of the coastally trapped Kelvin waves that explains the Angolan upwelling (Figure 2c). The coastal trapped waves have a semi-annual cycle of alternating upwelling (negative SLA) and downwelling (positive SLA) seasons (Ostrowski et al., 2009). The first downwelling occurs in March, followed by an upwelling in July–August (Figure 2c). The second downwelling occurs in October and ends with a weak upwelling in December–January (Figure 2c). In addition to coastal trapped waves, the mixing induced by internal tides can also contribute to the near-coastal Angola upwelling (Zeng et al., 2021). The satellite derived OSCAR current reveals an alongshore flow with alternating southward and northward velocity in the order of 10 cm/s. A southward OSCAR derived 11 cm/s mean flow occurs from January to March and from September to November while a weak 5 cm/s northward flow occurs during winter.

3.2. The Seasonal Mixed-Layer Salinity Budget

We now study the processes driving the SSS seasonal cycle along the Angolan coast.

Figure 3 presents the seasonal cycle of the mixed layer salinity and the salt budget along the Angola coast. In the model, the SSS is close to the averaged salinity in the mixed layer in which the model salt budget has been calculated. The mixed layer salinity has a semi-annual cycle characterized by a low-salinity of value 32.5 in February and October, respectively followed by increased salinity values up to 36 during the rest of the time,

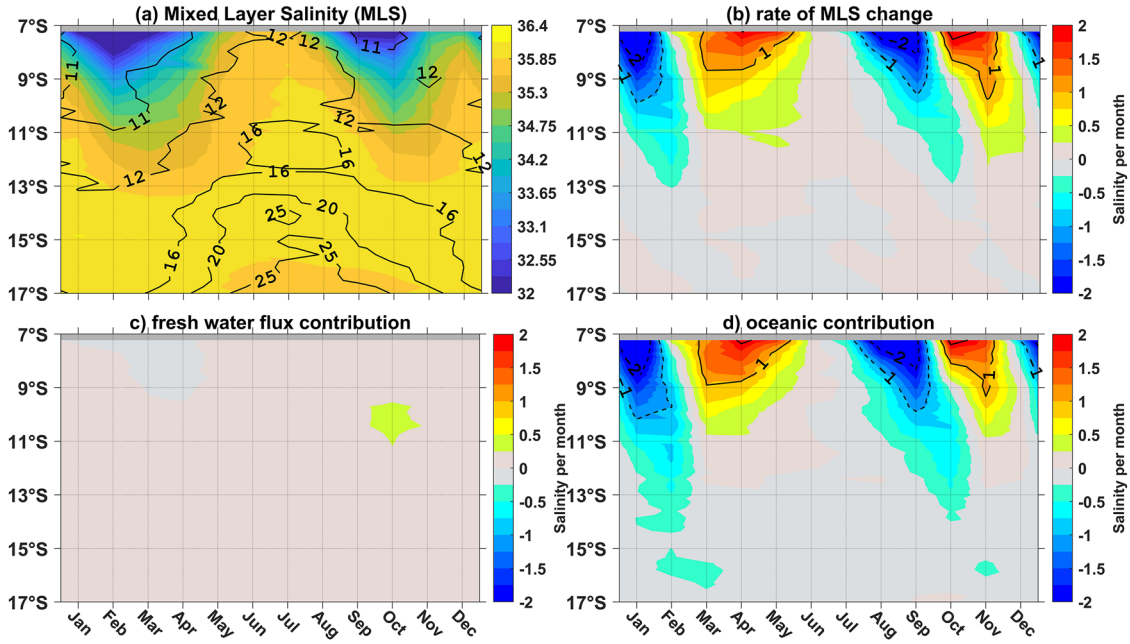

Figure 3. Latitude-time Hovmöller diagram of the model seasonal cycle of Mixed layer Salinity (a, -MSL-), the rate of the MLS change (b), the freshwater flux contribution (c) and the oceanic contribution (d) along the Angolan coast. The mixed layer depth along the coast is superimposed in contour line (a). Unit are m for mixed layer depth (a, contour line) and salinity per month for the rest of plots (b, c, d).

consistent with the observed SSS (Figures 2d and 2e). The monthly rate of SSS change is consistent with the seasonal cycle of SSS, with positive rates of salinity per month up to 2 corresponding to the increase of SSS and negative rates down to −2 corresponding to the decrease of SSS (Figures 3a and 3b). The rate of salinity change per month is negative from December to February and from July to October, in the range of −0.5 to − 2, leading to SSS decreases from January to March and from August to October, in the range of 36–32, respectively. But the rate of salinity change per month is positive from March to June and from October to November, in the range of 0.5–2, leading to an SSS increase from April to July and from November to December, in the range of 32–36, respectively. Along the North Angolan coast, the SSS varies between 32 and 36, while it varies between 35.4 and 36 along the South Angolan coast.

3.2.1. Salt Budget Analysis: Oceanic Vs. FWF Contributions

The mixed layer salinity budget is summarized in terms of FWF contribution (Figure 3c) and oceanic contribution (Figure 3d) to the salinity rate of change along the coast. The oceanic processes combine horizontal advection, vertical advection, vertical diffusion, lateral diffusion, and entrainment at the base of the mixed layer. The FWF combines Congo River discharge, precipitation and evaporation contributions to salinity change. The model presents a shallow mixed layer depth between 11 and 12 m in the North Angolan coast (Figure 3a) and a deep mixed layer depth between 16 and 25 m in the South Angola with a maximum depth during the winter Angola upwelling. Results show that the mixed-layer salinity along the coast is mostly maintained by oceanic processes (Figure 3d), where the horizontal advection of surface processes contribute to decrease the salinity per month by up to −2 (Figure 4a) while subsurface processes (vertical diffusion and vertical advection) contribute to increase the surface salinity per month up to 2. Subsurface processes increase mainly from January to April and from August to November in North Angola. The FWF contribution is comparatively weak with a salinity per month contribution of around 0.5 (Figure 3c) along the coast.

Finally, along the Angolan coast, the analysis highlights the horizontal advection as the main cause of low surface salinity water mainly in February–March and September–October, while the subsurface processes increase the SSS mainly from March to August and from November to December. In the next section, we will refine the analysis on the horizontal advection and subsurface processes.

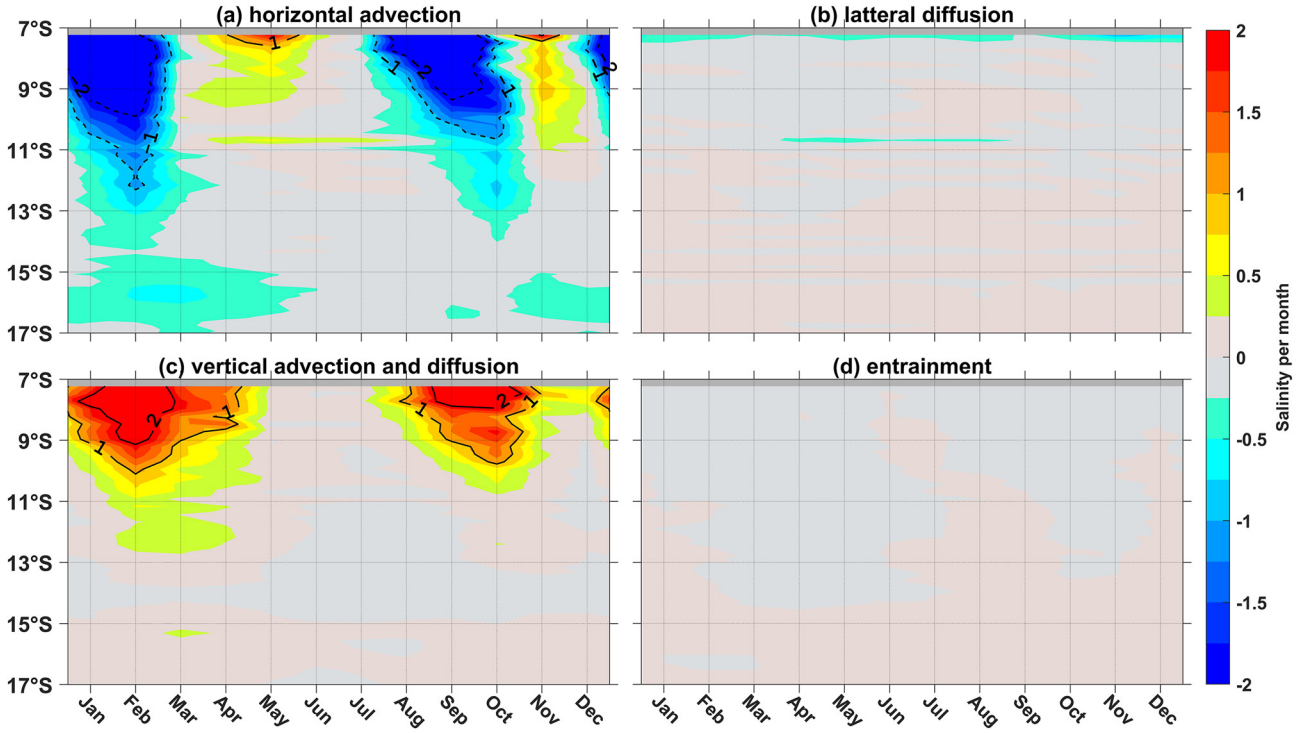

Figure 4. Latitude-time Hovmöller diagram of the horizontal advection (a), the lateral diffusion (b), the combined vertical advection and diffusion (c) and the entrainment (d) along the Angolan coast. Unit: Salinity per month.

3.2.2. Salt Budget Analysis: Horizontal Advection

Figure 5 presents the decomposition of horizontal advection into zonal (Figure 5a) and meridional (Figure 5b) components. Along the Angolan coast, horizontal advection is dominated by the meridional component. The Meridional advection peaks in February and September/October with values of salinity per month up to 2 (Figure 5b) when the horizontal advection also reaches the maximum of value (Figure 4a). The zonal advection contributes slightly to increase salinity per month with a range of 0.5–1 in the North Angola. The zonal advection also slightly contributes to decrease salinity per month in the order of 0.5 in South Angola (15°S–17°S). The result shows that the meridional component of horizontal advection contribution is more important to explain the low-salinity intrusion presented in Figure 2 along the Angolan coast during January–March and September–November. The zonal advection contribution is relatively minor compared to that meridional advection. However, the zonal advection slightly contributes to salinity per month in the order to 1 during February–

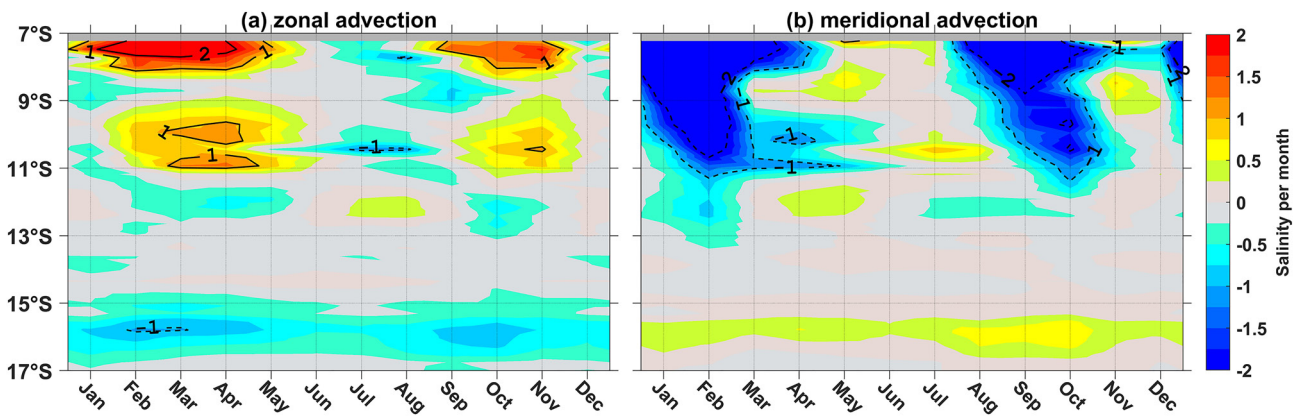

Figure 5. Latitude-time Hovmöller diagram of the zonal advection (a), the meridional advection (b) along the Angolan coast. Unit: Salinity per month.

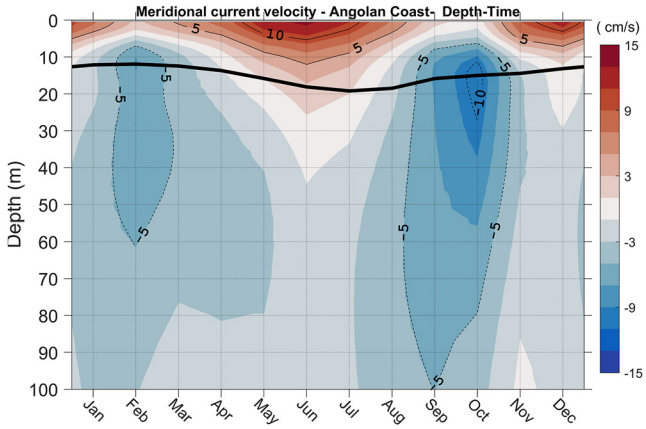

Figure 6. Depth-time Hovmöller diagram meridional current averaged over the entire Angolan Coast from the model. The black line represents the averaged mixed layer depth over the entire Angolan Coast. Equatorward current (red colour) and southward current (blue colour). Unit: cm/s.

April and September–November to counterbalance the meridional advection along the Angolan coast. In the next section, we will deepen our investigation on the meridional advection to see which parameter drives the seasonal cycle of meridional advection.

Figure 6 shows the relationship between the meridional advection and the meridional current to see whether the advection is driven by the current dynamics. Results show that the meridional current in the mixed layer is in phase with the meridional advection. The meridional current flows southward during January–February and September–October, and reverses into northward during March–August and November–December. The core of the southward current is located at the bottom of mixed layer at about 20 m with an intensity of −0.05 m/s in February and −0.10 m/s in October. During January–February and September–October, the southward current can therefore advect the low-salinity water from the Congo plume toward the Angolan coast. However, during March–August and November–December, the current reverses and brings back salty water northward with an intensity about 0.10 m/s during the winter. The southward current extends vertically down to 100 m depth while the northward current is close to the surface layer within the 0–10 m. The southward current is therefore part of the well-known geostrophic Angola Current. The northward surface current could be related to the surface wind stress or could be a coastal jet. Hence, the meridional flow is not symmetric. The poleward flow is at the subsurface while the equatorward flow is confined to the surface. This implies an asymmetric salt transport and may contribute to turbulence mixing.

At this stage, we can therefore conclude that the meridional current along Angolan coast is the main driver of the low-salinity intrusion at the Angolan coast.

In the model (Figure 2e), the southward low-salinity intrusion front, limited by isoline 35, is observed mostly in February–March and September–October. Compared to observation, the intrusion front is limited to North Angola in the model while the intrusion front reaches the South Angola in observation products (Figure 2e vs. Figure 2d). For instance, while the isoline 35 reaches around 14°S in the SMOS observation (Figure 2d), the isoline 35 reaches only 11°S in the model (Figure 2e). To understand the less southward extension of the low-salinity in model than observation, the satellite derived OSCAR current is compared to the model (Figure 2c vs. Figure 6). The semi-annual cycle of the near-surface current is observed in the satellite products, confirming the robustness of the model to reproduce the cycle of the near-surface current. Nevertheless, the model southward current in January–February and September–October is lower compared to satellite products while the model northward current in autumn and winter is stronger than satellite products (Figure 2c). For instance, along the Angolan coast, from January to February and September–October, the model current ranges between 0 and −0.05 m/s in the mixed layer while satellite derived currents range from 0 to −0.15 m/s. The lowest southerly extension of the model salinity intrusion front is then due to low model southward currents. Figures 7 and 8 compare the meridional velocity of the modeled current and the moored current located at 11°S off the Angolan coast. Current velocities have been measured by the moored ADCP between July 2013 and May 2021 from 45 to 450 m and was first reported by Kopte et al. (2017) and recently updated by Imbol Koungue et al. (2021) to present the direct velocity observations of Angolan Current at 11°S. The climatology of the moored current is based on the full available mooring data (2013–2021) and the model current is based on the period from 1982 to 2015 (Figure 7). In Figure 8, we present the current monthly mean average for the common period 2013–2015 of the mooring and model. At seasonal timescale, between the depths of 50 and 100 m, the southward current previously identified to have a role in the advection of low-salinity water is also observed in the mooring data with maxima in February/March and September/October. This southward current extends to the surface in the model, however this feature is not present in the mooring measured current, as the ADCP mounted at depth on the mooring cable measures the current velocity from the bottom to 45 m only below the surface. In September, a southward current of 10 cm/s extends to 250 m of depth in the model as well as in the mooring data. Between the depths of 150 and 250 m, a deep northward current is simulated by the model and also present in the mooring with a remarkable intensity of 10 cm/s in November which extends to 50 m below the surface. Despite the short

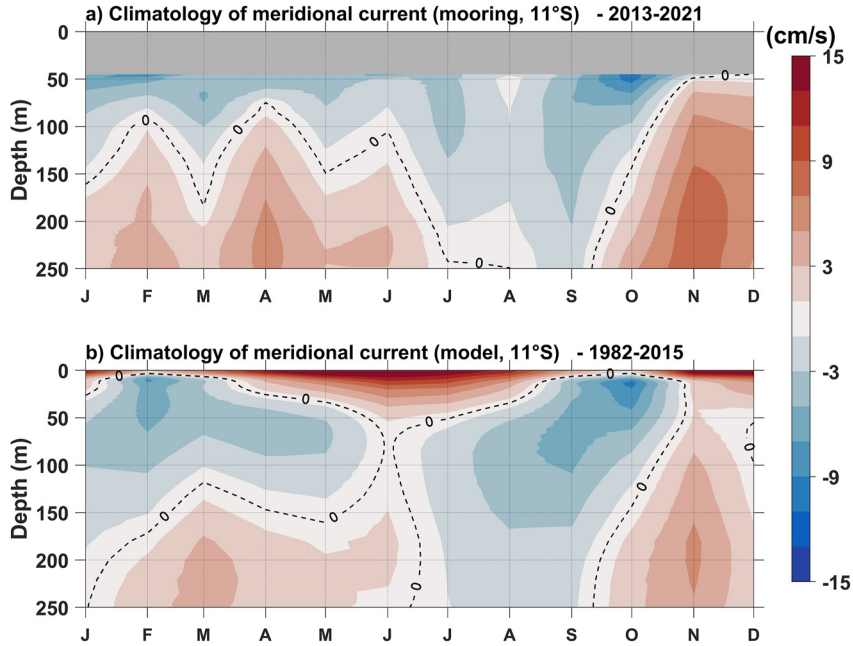

Figure 7. Seasonal cycle of the meridional velocity of the modeled current (b) and the moored current (a) located at 11°S off the Angolan coast. The moored current climatology is computed over the full available mooring data (2013 to 2021) and the modeled current is computed over the period 1982 to 2015. Unit: cm/s.

common period, the simulated current reproduces the observed monthly current relatively well (Figure 8). The subsurface southward currents velocities observed in February/March and September/October of 2013, 2014, and 2015 are identified in the model as well as the subsurface northward current velocity of the model in November/December of 2013, 2014, and 2015.

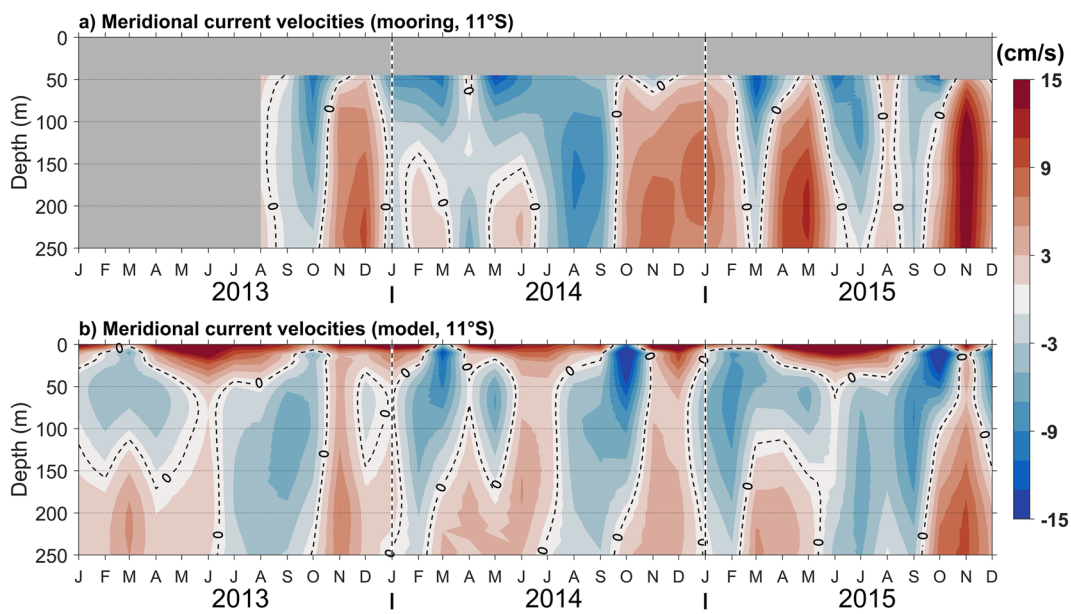

Figure 8. The monthly mean of the meridional current computed on the common period 2013 to 2015 of the mooring (a) and model (b) data located at 11°S off the Angolan coast. Unit: cm/s.

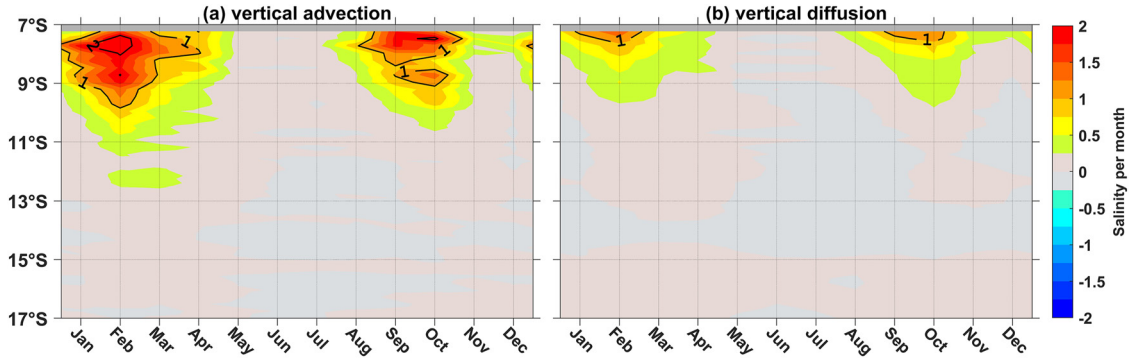

Figure 9. Latitude-time Hovmöller diagram of the vertical advection (a), the vertical diffusion (b) along the Angolan coast. Unit: Salinity per month.

3.2.3. Salt Budget Analysis: Subsurface Processes

In the previous section (Figure 4), we show that subsurface processes are the main driver of the salinization at the surface along the Angolan coast, especially from January to April and from August to November, when the meridional advection weakens. In this section, we want to estimate the contribution of each component of subsurface processes.

Figure 9 presents the decomposition subsurface processes into vertical advection and vertical diffusion. Results show that both vertical advection and diffusion are important to explain the salinization in the mixed layer. The vertical advection is stronger than diffusion and extends southward until 11°S while the vertical diffusion reaches only 9°S.

The contribution of vertical advection accounts for 0.18 of salinity change per month while the vertical diffusion is about 0.10 along the northern coast.

As subsurface processes are dominated by change in the vertical advection that results from the combination of vertical current and vertical salinity gradient structure, we will now explore the behavior of each component of the vertical advection.

Figure 10 presents the seasonal cycle of vertical salinity and current averaged along the coast. The vertical current velocity ranges between -1×10^{-3} and 1×10^{-3} cm/s. The current velocity shows a semi-annual cycle, with a first maximum of 0.75×10^{-3} cm/s in July and a second maximum of 0.5×10^{-3} cm/s in November/December.

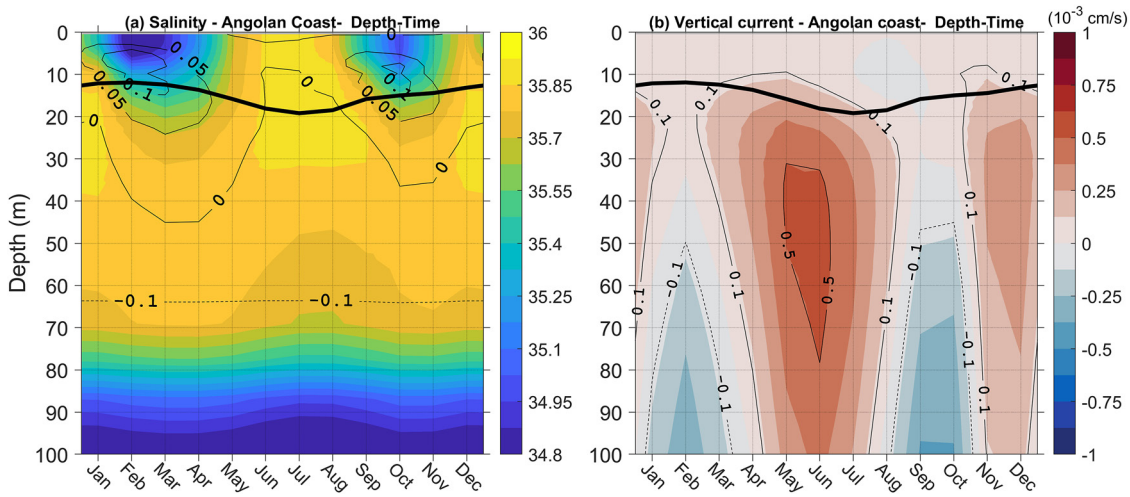

Figure 10. Depth-time Hovmöller diagram of salinity (a, shading colour), vertical salinity gradient (a, thin black contour line) and vertical current (b, Positive value: upward current) averaged over the entire Angolan Coast from the model. The black line represents the averaged mixed layer depth over the entire Angolan Coast. Units: Salinity per meter for vertical salinity gradient and cm/s for current.

Along the coast, the core of the current velocity in July is close to the mixed layer depth. The mixed layer depth is shallower along the North Angolan coast (about 10 m deep) than along the South Angolan coast (about 25 m deep). Both maxima in vertical current (respectively in July and December) do not match with the strong vertical advection contribution (respectively in February and October, Figure 9a), meaning that the observed salinization is not predominantly related to the vertical current changes. The vertical salinity gradient at the bottom of mixed layer depth is positive over the year (salinity is decreasing upwards, with positive depth coordinates downwards) with a maximum in February/March and September/October (Figure 10a), except in July to August when the vertical salinity is homogenous and therefore does not present any vertical stratification. Despite the low velocity of vertical current during the February/March and September/October, the strong vertical salinity stratification per meter of value around 0.1 (dS/dz) during this period is enough for the weak vertical velocity of value 0.25×10^{-3} cm/s to bring salty water toward the surface and therefore explains the important contribution of the vertical advection to the salinization within the mixed layer.

4. Discussion and Conclusion

In this study, the seasonal cycle of the SSS along the Angolan Coast is investigated using observations and a regional ocean model. The model is shown to reproduce the main characteristic of the seasonal cycle of SSS along the Angolan coast. The model reproduces the freshwater discharge signature of the Congo River plume, a lower salinity in February/March and October/November and a higher salinity from March to September. Along the North Angolan coast, the standard deviation value of the observed SSS variability is of the order of 1.37 psu while it is 0.56 psu along the South Angola coast. The analysis of the mixed-layer salinity budget from the model reveals that the seasonal cycle of SSS is mainly driven by oceanic processes. The decomposition of oceanic processes show that the meridional advection, the vertical advection, and the vertical diffusion drive the seasonal cycle of SSS along the Angolan coast. The meridional advection is controlled by the meridional current, which brings low-salinity water from the coastal water off Congo River region toward South Angola in February/March and October/November. The meridional current corresponds to the Angola Current that flows along the coast and may transport nutrients southward (Kopte et al., 2017; Ostrowski et al., 2009). The vertical advection and vertical diffusion contribute only to increasing the SSS from February to April and from September to November along the Angolan coast, contrary to the Congolese area, where both vertical processes contribute to increase and decrease the salinity (Berger et al., 2014; Da-Allada et al., 2014). Along the Angolan coast, changes in the divergence of the vertical advective salt flux is more related to changes in the salinity gradient and less to the vertical velocities. The vertical velocity peaks during the Angolan upwelling season when the meridional advection weakens along the coast. The vertical stratification is related to the low-salinity intrusion at the Angolan coast that creates a strong vertical salinity gradient with a low-salinity at the surface layer and a high salinity at the subsurface. During the austral winter, when the Angola upwelling is the most intense, the strong vertical current cannot bring much salty water to the surface, since the vertical stratification of salinity is low during the upwelling season (Figure 10a). The vertical advection then dominates the vertical processes along the coast and this result is consistent with previous results done off the Congolese coast (Berger et al., 2014; Da-Allada et al., 2014). These results support the complementary behavior of surface and subsurface processes to explain the seasonal cycle of SSS along the Angolan coast. The source of the observed low-salinity intrusion off the Angolan coast is the Congo River plume that discharges freshwater into the ocean. The salinity impact on the Angola upwelling intensity is not really documented. During the major upwelling in austral winter, the model surface salinity variation along the Angola coast is very weak and could not significantly affect in turn the upwelling. However, in austral autumn and spring, when the low-salinity intrusion is observed, there could be an impact of this low-salinity on the intensity of the weak upwelling that appears in austral spring. Indeed, the low-salinity intrusion could inhibit the upwelling by creating a barrier layer (Dossa et al., 2019; Materia et al., 2012). However, Martins and Stammer (2022) do not find a correlation between the plume patterns and the different upwellings strengths in the SMOS satellite data. Using regional ocean model experiments with or without River discharge, Alory et al. (2021) have shown that the low-salinity related to the Niger River freshwater discharge warms the upwelling tongue by up to 1°C in the north Gulf of Guinea. This recent model experiment could be applied to investigate the impact of Congo River discharge on the Angola upwelling. Zeng et al. (2021) suggest that the mixing induced by internal tides can contribute to the near-coastal Angola upwelling and maybe changes in ocean salinity. To improve our analysis related to vertical mixing, a new high-resolution simulation of the NEMO model that includes tidal mixing should be performed to quantify the contribution of tidal mixing. As

the low-salinity observed along South Angola coast comes from Congo River plume, additional investigations are needed to better estimate the propagation speed of the low-salinity signal toward the southern Angola.

Data Availability Statement

All the satellite derived, reanalyze and in situ data sets used in this study are publicly available. The following lists the data sets and URLs from which we downloaded them. Free Registration charge is required for access ERA5 and AVISO. SMOS: https://data.catds.fr/cecos-locean/Ocean_products/L3_DEBIAS_LOCEAN/L3_DEBIAS_LOCEAN_v7/debiasedSSS_18days_v7/. OISST: https://psl.noaa.gov/data/gridded/data.noaa.oisst.v2.highres.html. OSCAR: https://podaac.jpl.nasa.gov/dataset/OSCAR_L4_OC_FINAL_V2.0. AVISO: http://www.aviso.altimetry.fr. ERA5: https://cds.climate.copernicus.eu/#!/search?text=ERA5&type=dataset. Mooring data: https://doi.pangaea.de/10.1594/PANGAEA.939249.

Acknowledgments
This work is part of the TRIATLAS European project (South and Tropical Atlantic climate-based marine ecosystem prediction for sustainable management; H2020 Grant agreement No 817578) which supported the post-doctoral fellowship funded by Nansen Tutu Center for Marine Environmental Research, Department of Oceanography, University of Cape Town, Cape Town, South Africa. Additional funding came from the NRF Sarchi Chair on Ocean Atmosphere Modeling, the Belmont Forum CRA Transdisciplinary Research for Ocean Sustainability (Ocean 2018), EXEBUS: Ecological and Econmic impacts of the intensification of extreme events in the Benguela Upwelling System and the Research Council of Norway PCO2 project No 309347. The authors thank Peter Brandt and Anicet Rodrigue Imbol Koungue for providing the mooring data. The authors also thank the two anonymous reviewers for their helpful comments.

References

Alory, G., Da-Allada, C. Y., Djakouré, S., Dadou, I., Jouanno, J., & Loemba, D. P. (2021). Coastal upwelling limitation by onshore geostrophic flow in the Gulf of Guinea around the Niger River plume. *Frontiers in Marine Science*, *7*, 607216. https://doi.org/10.3389/fmars.2020.607216

Awo, F. M., Alory, G., Da-Allada, C. Y., Delcroix, T., Jouanno, J., Kestenare, E., & Baloïtcha, E. (2018). Sea surface salinity signature of the tropical Atlantic interannual climatic modes. *Journal of Geophysical Research: Oceans*, *123*(10), 7420–7437. https://doi.org/10.1029/2018jc013837

Bachèlery, M. L., Illig, S., & Dadou, I. (2016). Interannual variability in the southeast Atlantic Ocean, focusing on the Benguela upwelling system: Remote vs. local forcing. *Journal of Geophysical Research: Oceans*, *121*(1), 284–310. https://doi.org/10.1002/2015JC011168

Berger, H., Tréguier, A., Perenne, N., & Talandier, C. (2014). Dynamical contribution to sea surface salinity variations in the eastern Gulf of Guinea based on numerical modeling. *Climate Dynamics*, *43*(11), 3105–3122. https://doi.org/10.1007/s00382-014-2195-4

Blamey, L. K., Shannon, L. J., Bolton, J. J., Crawford, R. J., Dufois, F., Evers-King, H., et al. (2015). Ecosystem change in the southern Benguela and the underlying processes. *Journal of Marine Systems*, *144*, 9–29. https://doi.org/10.1016/j.jmarsys.2014.11.006

Bonjean, F., & Lagerloef, G. S. (2002). Diagnostic model and analysis of the surface currents in the tropical Pacific Ocean. *Journal of Physical Oceanography*, *32*(10), 2938–2954. https://doi.org/10.1175/1520-0485(2002)032<2938:dmaaot>2.0.co;2

Boutin, J., Vergely, J.-L., & Khvorostyanov, D. (2022). SMOS SSS L3 maps generated by CATDS CEC LOCEAN. debias V7.0. SEANOE. https://doi.org/10.17882/52804#91742

Boutin, J., Vergely, J. L., Marchand, S., D'Amico, F., Hasson, A., Kolodziejczyk, N., et al. (2018). New SMOS sea surface salinity with reduced systematic errors and improved variability. *Remote Sensing of Environment*, *214*, 115–134. https://doi.org/10.1016/j.rse.2018.05.022

Camara, I., Kolodziejczyk, N., Mignot, J., Lazar, A., & Gaye, A. T. (2015). On the seasonal variations of salinity of the tropical Atlantic mixed layer. *Journal of Geophysical Research: Oceans*, *120*, 4441–4462. https://doi.org/10.1002/2015jc010865

Carr, M.-E., & Kearns, E. J. (2003). Production regimes in four eastern boundary current systems. *Deep-Sea Research Part II: Topical Studies in Oceanography*, *50*, 3199–3221. https://doi.org/10.1016/j.dsr2.2003.07.015

Da-Allada, C. Y., Alory, G., Du Penhoat, Y., Kestenare, E., Durand, F., & Hounkonnou, N. M. (2013). Seasonal mixed-layer salinity balance in the tropical Atlantic Ocean: Mean state and seasonal cycle. *Journal of Geophysical Research: Oceans*, *118*(1), 332–345. https://doi.org/10.1029/2012JC008357

Da-Allada, C. Y., Du Penhoat, Y., Jouanno, J., Alory, G., & Hounkonnou, N. M. (2014). Modeled mixed-layer salinity balance in the Gulf of Guinea: Seasonal and interannual variability. *Ocean Dynamics*, *64*(12), 1783–1802. https://doi.org/10.1007/s10236-014-0775-9

Da-Allada, C. Y., Jouanno, J., Gaillard, F., Kolodziejczyk, N., Maes, C., Reul, N., & Bourlès, B. (2017). Importance of the equatorial undercurrent on the sea surface salinity in the eastern equatorial Atlantic in boreal spring. *Journal of Geophysical Research: Oceans*, *122*(1), 521–538. https://doi.org/10.1002/2016JC012342

Dai, A., & Trenberth, K. E. (2002). Estimates of freshwater discharge from continents: Latitudinal and seasonal variations. *Journal of Hydrometeorology*, *3*(6), 660–687. https://doi.org/10.1175/1525-7541(2002)003<0660:EOFDFC>2.0.CO;2

Dossa, A. N., Da-Allada, C. Y., Herbert, G., & Bourlès, B. (2019). Seasonal cycle of the salinity barrier layer revealed in the northeastern Gulf of Guinea. *African Journal of Marine Science*, *41*(2), 163–175. https://doi.org/10.2989/1814232x.2019.1616612

Dussin, R., Barnier, B., & Brodeau, L. (2016). *The making of Drakkar forcing set DFS5*. DRAKKAR/MyOcean Report 01-04-16, LGGE.

ESR, & Dohan, K. (2022). Ocean Surface Current Analyses Real-time (OSCAR) Surface Currents - Final 0.25 Degree (Version 2.0). Ver. 2.0. PO. [Dataset]. DAAC. https://doi.org/10.5067/OSCAR-25F20

Ferry, N., Parent, L., Garric, G., Bricaud, C., Testut, C.-E., Le Galloudec, O., et al. (2012). GLORYS2V1 global ocean reanalysis of the altimetric era (1992–2009) at mesoscale. *Mercator Quarterly Newsletter*, *44*, 29–39. Retrieved from http://www.mercator-ocean.fr/eng/actualitesagenda/newsletter

Florenchie, P., Reason, C. J. C., Lutjeharms, J. R. E., Rouault, M., Roy, C., & Masson, S. (2004). Evolution of interannual warm and cold events in the southeast Atlantic Ocean. *Journal of Climate*, *17*(12), 2318–2334. https://doi.org/10.1175/1520-0442(2004)017<2318:EOIWAC>2.0.CO;2

Hellerman, S. (1980). Charts of the variability of the wind stress over the tropical Atlantic. In G. Siedler, J. D. Woods, & W. Düing (Eds.), *Oceanography and surface layer meteorology in the B/C scale* (pp. 63–75). Pergamon. https://doi.org/10.1016/B978-1-4832-8366-1.50022-4

Hernandez, O., Jouanno, J., Echevin, V., & Aumont, O. (2017). Modification of sea surface temperature by chlorophyll concentration in the Atlantic upwelling systems. *Journal of Geophysical Research: Oceans*, *122*, 5367–5389. https://doi.org/10.1002/2016JC012330

Hersbach, H., Bell, B., Berrisford, P., Hirahara, S., Horanyi, A., Munoz-Sabater, J., et al. (2020). The ERA5 global reanalysis. *Quarterly Journal of the Royal Meteorological Society*, *146*, 1999–2049. https://doi.org/10.1002/qj.3803

Houndegnonto, O. J., Kolodziejczyk, N., Maes, C., Bourlès, B., Da-Allada, C. Y., & Reul, N. (2021). Seasonal variability of freshwater plumes in the eastern Gulf of Guinea as inferred from satellite measurements. *Journal of Geophysical Research: Oceans*, *126*, e2020JC017041. https://doi.org/10.1029/2020JC017041

Hutchings, L., van der Lingen, C. D., Shannon, L. J., Crawford, R. J. M., Verheye, H. M. S., Bartholomae, C. H., et al. (2009). The Benguela Current: An ecosystem of four components. Prog. Oceanogr., Eastern Boundary Upwelling Ecosystems: Integrative and Comparative

Approaches: Integrative and comparative approaches, 2–8 June 2008, Las Palmas, Gran Canaria, Spain Eastern Boundary Upwelling Ecosystems Symposium 83, (pp. 15–32). https://doi.org/10.1016/j.pocean.2009.07.046

Illig, S., Bachèlery, M. L., & Lübbecke, J. F. (2020). Why do Benguela Niños lead Atlantic Niños? *Journal of Geophysical Research: Oceans*, *125*(9), e2019JC016003.

Imbol Koungue, R. A., Brandt, P., Lübbecke, J., Prigent, A., Martins, M., & Rodrigues, R. (2021). The 2019 Benguela Niño. *Frontiers in Marine Science*, *8*, 800103. https://doi.org/10.3389/fmars.2021.800103

Imbol Koungue, R. A., Illig, S., & Rouault, M. (2017). Role of interannual Kelvin wave propagations in the equatorial Atlantic on the Angola Benguela Current system. *Journal of Geophysical Research: Oceans*, *122*(6), 4685–4703. https://doi.org/10.1002/2016JC012463

Imbol Koungue, R. A., Rouault, M., Illig, S., Brandt, P., & Jouanno, J. (2019). Benguela Niños and Benguela Niñas in forced ocean simulation from 1958 to 2015. *Journal of Geophysical Research: Oceans*, *124*, 5923–5951. https://doi.org/10.1029/2019JC015013

Jouanno, J., Hernandez, O., & Sanchez-Gomez, E. (2017). Equatorial Atlantic interannual variability and its relation to dynamic and thermodynamic processes. *Earth System Dynamics*, *8*(4), 1061–1069. https://doi.org/10.5194/esd-8-1061-2017

Jouanno, J., Marin, F., du Penhoat, Y., Sheinbaum, J., & Molines, J.-M. (2011). Seasonal heat balance in the upper 100 m of the equatorial Atlantic Ocean. *Journal of Geophysical Research*, *116*, C09003. https://doi.org/10.1029/2010JC006912

Kolodziejczyk, N., Boutin, J., Vergely, J.-L., Marchand, S., Martin, N., & Reverdin, G. (2016). Mitigation of systematic errors in SMOS sea surface salinity. *Remote Sensing of Environment*, *180*, 164–177. https://doi.org/10.1016/j.rse.2016.02.061

Kopte, R., Brandt, P., Dengler, M., Tchipalanga, P. C., Macuérie, M., & Ostrowski, M. (2017). The Angola Current: Flow and hydrographic characteristics as observed at 11°S. *Journal of Geophysical Research: Oceans*, *122*, 1177–1189. https://doi.org/10.1002/2016JC012374

Large, W. G., & Yeager, S. G. (2004). *Diurnal to decadal global forcing for ocean sea ice models: The data sets and flux climatologies*. Rep. NCAR/TN-460+STR. Natl Cent for Atmos Res. http://dx.doi.org/10.5065/D6KK98Q6

Lübbecke, J. F., Böning, C. W., Keenlyside, N. S., & Xie, S.-P. (2010). On the connection between Benguela and equatorial Atlantic Niños and the role of the South Atlantic anticyclone. *Journal of Geophysical Research*, *115*, C09015. https://doi.org/10.1029/2009JC005964

Lübbecke, J. F., Brandt, P., Dengler, M., Kopte, R., Lüdke, J., Richter, I., et al. (2019). Causes and evolution of the southeastern tropical Atlantic warm event in early 2016. *Climate Dynamics*, *53*(1), 261–274. https://doi.org/10.1007/s00382-018-4582-8

Madec, G., & the NEMO team. (2016). NEMO ocean engine: Note du Pôle de modélisation de l'Institut Pierre-Simon Laplace No 27. Retrieved from http://www.nemo-ocean.eu/doc

Martins, M. S., & Stammer, D. (2022). Interannual variability of the Congo River plume-induced sea surface salinity. *Remote Sensing*, *14*, 1013. https://doi.org/10.3390/rs14041013

Materia, S., Gualdi, S., Navarra, A., & Terray, L. (2012). The effect of Congo River freshwater discharge on eastern equatorial Atlantic climate variability. *Climate Dynamics*, *39*, 2109–2125. https://doi.org/10.1007/s00382-012-1514-x

Moroshkin, K. V., Bunov, V. A., & Bulatov, R. P. (1970). Water circulation in the eastern South Atlantic Ocean. *Oceanology*, *10*, 27–34.

Ostrowski, M., Da Silva, J. C., & Bazik-Sangolay, B. (2009). The response of sound scatterers to El Niño-and La Niña-like oceanographic regimes in the southeastern Atlantic. *ICES Journal of Marine Science*, *66*(6), 1063–1072. https://doi.org/10.1093/icesjms/fsp102

Reynolds, R. W., Rayner, N. A., Smith, T. M., Stokes, D. C., & Wang, W. (2002). An improved in situ and satellite SST analysis for climate. *Journal of Climate*, *15*, 1609–1625.

Reynolds, R. W., Smith, T. M., Liu, C., Chelton, D. B., Casey, K. S., & Schlax, M. G. (2007). Daily high-resolution-blended analyses for sea surface temperature. *Journal of Climate*, *20*, 5473–5496. https://doi.org/10.1175/2007JCLI1824.1

Rouault, M. (2012). Bi-annual intrusion of tropical water in the northern Benguela upwelling. *Geophysical Research Letters*, *39*(12). https://doi.org/10.1029/2012GL052099

Shannon, L. V., Boyd, A. J., Brundrit, G. B., & Taunton-Clark, J. (1986). On the existence of an El Niño-type phenomenon in the Benguela system. *Journal of Marine Research*, *44*, 495–520. https://doi.org/10.1357/002224086788403105

Sowman, M., & Cardoso, P. (2010). Small-scale fisheries and food security strategies in countries in the Benguela Current Large Marine Ecosystem (BCLME) region: Angola, Namibia, and South Africa. *Marine Policy*, *34*, 1163–1170. https://doi.org/10.1016/j.marpol.2010.03.016

Zeng, Z., Brandt, P., Lamb, K. G., Greatbatch, R. J., Dengler, M., Claus, M., & Chen, X. (2021). Three-dimensional numerical simulations of internal tides in the Angolan upwelling region. *Journal of Geophysical Research: Oceans*, *126*, e2020JC016460. https://doi.org/10.1029/2020JC016460